PHYSICAL REVIEW B **81**, 140502(R) (2010)

Magnetic form factor of $SrFe_2As_2$: Neutron diffraction measurements

W. Ratcliff II,[1,*] P. A. Kienzle,[1] Jeffrey W. Lynn,[1] Shiliang Li,[2,4] Pengcheng Dai,[2,3,4] G. F. Chen,[4] and N. L. Wang[4]
[1]*NIST Center for Neutron Research, National Institute of Standards and Technology, Gaithersburg, Maryland 20899, USA*
[2]*Department of Physics and Astronomy, University of Tennessee, Knoxville, Tennessee 37996, USA*
[3]*Neutron Scattering Science Division, Oak Ridge National Laboratory, Oak Ridge, Tennessee 37831, USA*
[4]*Beijing National Laboratory for Condensed Matter Physics, Institute of Physics, Chinese Academy of Sciences, Beijing 100080, People's Republic of China*

(Received 12 January 2010; revised manuscript received 14 March 2010; published 9 April 2010)

Neutron diffraction measurements have been carried out to investigate the magnetic form factor of the parent $SrFe_2As_2$ system of the iron-based superconductors. The general feature is that the form factor is approximately isotropic in wave vector, indicating that multiple *d* orbitals of the iron atoms are occupied as expected based on band theory. Inversion of the diffraction data suggests that there is some elongation of the spin density toward the As atoms. We have also extended the diffraction measurements to investigate a possible jump in the *c*-axis lattice parameter at the structural phase transition but find no detectable change within the experimental uncertainties.

DOI: 10.1103/PhysRevB.81.140502 PACS number(s): 74.70.Xa, 75.25.−j, 64.60.Ej, 61.05.F−

I. INTRODUCTION

The nature of the magnetic moment and the spin configuration of the long-range antiferromagnetic order in the iron-based pnictide superconductor class of materials is a topic of great current interest. Antiferromagnetic order develops at or just below a structural distortion that breaks the tetragonal symmetry.[1] In the distorted *a*-*b* plane the spins align antiparallel along the longer *a*-axis while they align parallel along the *b* axis. Hence the distortion plays an essential role in the magnetic structure since this magnetic configuration does not have tetragonal symmetry, and a number of theories suggest that the mechanism of the structural distortion is magnetic.[2–4] We have carried out quantitative measurements of the magnetic Bragg intensities for $SrFe_2As_2$ to determine the magnetic form factor, which is directly related to the magnetization density in the unit cell of the crystal through Fourier inversion. We find that the dominant spin density resides on the iron as expected and is approximately isotropic indicating that multiple *d* orbitals are occupied.[4] This approximate isotropy strongly contrasts with other $S=\frac{1}{2}$ magnets such as for the undoped cuprate superconductors systems[5] as well as K_2IrCl_6,[6] where the form factor is highly anisotropic and has orbital bonding character. In the present system there also is some modest anisotropy, and this appears to originate from iron-arsenic bonding.

II. EXPERIMENTAL PROCEDURES

Neutron diffraction measurements were carried out to study the structural transition and magnetic order in this material. Data were collected on the BT-9 triple-axis spectrometer at the NIST Center for Neutron Research. The neutron energies were fixed through the use of pyrolytic graphite (PG) (002) monochromator and analyzer. Measurements of the magnetic form factor were carried out at 14.7 meV, and also with 35 meV to access more reflections and to evaluate the possible role of extinction, which was found not to be a problem. Relatively relaxed Söller collimations of 40′-23′-S-40′-120′ full width at half maximum (FWHM) were employed. To determine the variation of the *c*-axis lattice parameter through the structural phase transition, tight Söller collimations of 10′-10′-S-10′-80′ FWHM were utilized at a neutron energy of 14.7 meV. PG filters were placed both before and after the sample to suppress higher order wavelengths to negligible levels. The single crystal measured was the same one used in a previous study, with orthorhombic lattice parameters $a \approx b \approx 5.57$ Å and $c \approx 12.29$ Å.[7] Magnetic reflections were measured in the $[H,0,L]$ zone in a helium cryostat. Uncertainties where indicated are statistical in origin and represent one standard deviation.

III. FORM FACTOR RESULTS AND DISCUSSION

The canonical equation for the differential cross section describing the coherent elastic scattering of neutrons from magnetically ordered crystals in the ground state is given by[6,8,9]

$$\frac{d\sigma}{d\omega} \propto N_M \frac{2\pi^3}{V_M} \sum_{\vec{G}_M} \delta(\vec{Q} - \vec{G_M}) |\vec{F_M}(\vec{G_M})|^2 \qquad (1)$$

where N_M is the number of magnetic unit cells in the crystal and V_M is the volume of the magnetic unit cell. For a simple collinear magnetic structure the vector magnetic structure factor $\vec{F}_M$ is related to the scalar magnetic structure factor by

$$|\vec{F}_M(G)|^2 = \left(\frac{\gamma \mu_0 e^2}{4\pi m_e}\right)^2 \langle 1 - (\hat{G} \cdot \hat{M})^2 \rangle |F_M(G)|^2 \qquad (2)$$

where the neutron-electron coupling constant in parenthesis is -0.27×10^{-14} m, $\hat{G}$ and $\hat{M}$ are unit vectors in the direction of the reciprocal-lattice vector $\vec{G}$ and the spin direction, respectively, and the scalar structure factor is

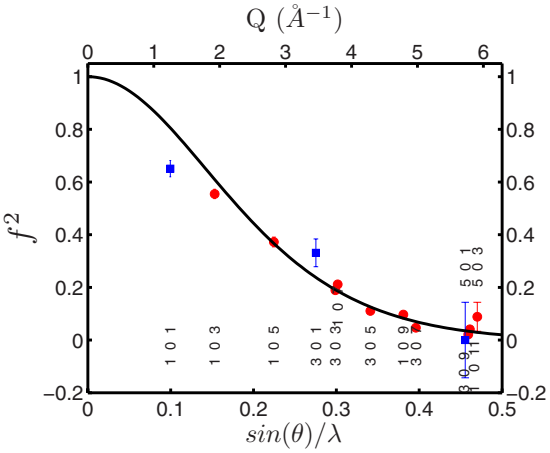

FIG. 1. (Color online) Measurement of the square of the magnetic form factor as a function of $Q=4\pi \sin(\theta)/\lambda$. Circles denote reflections which are predominantly along (0,0,L). Squares represent reflections which are predominantly along (H,0,0). The solid curve shows the form factor of metallic iron (Ref. 4). Error bars are statistical in nature and represent one standard deviation.

$$F_M(G) = \sum_{j=1}^{N} \langle \mu_j \rangle f_j(G) e^{iG \cdot r_j} e^{-W}. \quad (3)$$

Here $\langle \mu_j \rangle$ is the thermal average of the ordered magnetic moment of the j^{th} atom in the unit cell, r_j is the position of the j^{th} atom in the magnetic unit cell, $f_j(\vec{Q})$ is the scalar magnetic form factor of the j^{th} atom in the cell, and the sum j ranges over all atoms in the unit cell. The (scalar) magnetic form factor is the quantity of direct interest here, and is the Fourier transform of the magnetization density associated with each atom.

In an earlier work we determined the magnetic structure and order parameter of $SrFe_2As_2$, which consists of antiparallel Fe spins along the a and c directions and parallel spins along b, with the spin direction along a.[7] The effects of crystallographic twinning are also discussed in that work. Here we take this spin arrangement as a starting point and extract the magnetic form factor. The results, based on fits to the integrated intensities measured at base temperature (4 K) of 13 independent magnetic reflections (indexed on the basis of the orthorhombic cell), are shown in Fig. 1. The solid curve represents the tabulated isotropic form factor for metallic Fe,[10] and the general overall agreement with the measurements indicates that the magnetization density is isotropic to a good approximation. Note in particular that reflections of predominately (0,0,L) character (represented by circles in Fig. 1) and those of (H,0,0) character (represented by squares) both follow a similar curve, indicating that the form factor is approximately isotropic. This behavior is in stark contrast to what was found in other $S=\frac{1}{2}$ systems such as the high-T_C cuprate family[5] and K_2IrCl_6,[6] where the magnetic form factor originates from a single type of orbital that renders them highly directional.

Further perspective of the spatial distribution of the magnetization density can be gained through a real-space representation via direct Fourier inversion of the form factor, if sufficient experimental data are taken. Our data, which extend to higher Q than other measurements of the form factor,[19] allow for such a reconstruction. In measurements of neutron intensities we only determine the magnitude of the structure factor, not its phase. In the present case the structure factors are real since we have a centrosymmetric structure, and we assign the sign of the structure factor based on our previously determined spin structure. The results of the Fourier inversion are shown in Fig. 2(a). As our data were obtained in the (H,0,L) zone, we obtain the projection of the magnetization density along the b axis of the crystal. In the figure, we overlay the density plot with the atomic structure. The two gray (color) levels represent positive and negative magnetizations and show that we recover the antiferromagnetic structure of our original model. However, we notice that there are relatively long tails of the magnetization density which suggest hybridization along the a axis with the As atoms above and below the plane containing the Fe atoms in this projection.

One question to address is whether sufficient data have been measured to obtain a reliable magnetization density. To test the reliability of the inversion and possible effects of peaks that were not obtained experimentally, we calculated form factor values, including $K \neq 0$ (out-of-scattering-plane) reflections as well as higher Q reflections. The calculated values were based on the known magnetic structure and an assumed spherical Fe form factor. Then this extended set of form factor data was Fourier inverted. Figure 2(b) shows a cut of the real-space a-c plane that contains the Fe, which can be directly compared with the projection in Fig. 2(a). We see that the magnetization densities in the two plots are quite similar, demonstrating that the features obtained from the actual data are robust against termination effects and the absence of $K \neq 0$ data.

An alternative to the direct Fourier inversion of the data to obtain the magnetization density is to carry out a maximum entropy[11] reconstruction of the moment density. The basic idea behind maximum entropy is that there may be a number of possible moment densities that fit the form factor data equally well within the experimental uncertainties. Thus to obtain a representative moment density, the strategy is to search for moment densities which maximize entropy, while constrained to minimize the fit to the data. This technique picks the most likely magnetization density consistent with the data. While there are many different algorithms for obtaining the maximum entropy solution, we used a program called ALGENCAN (see Ref. 12) to treat the maximum entropy reconstruction as a constrained optimization problem. The results of the maximum entropy approach are shown in Fig. 2(c). Here, we find the same type of anisotropy in the moment density, although not as pronounced as in the direct Fourier reconstruction. Note that in Fig. 2 the maximum magnetizations have been normalized to be the same in each part so that in Fig. 2(c) the magnetization density falls off more quickly than in Figs. 2(a) and 2(b). We remark that the results in Fig. 2(c) are consistent with those obtained using the PRIMA maximum entropy program,[13] and note that both reconstructions suggest that the Fe magnetization density tends to be elongated toward the As atoms. In all reconstructions, we also note that there is a modulation of the moment

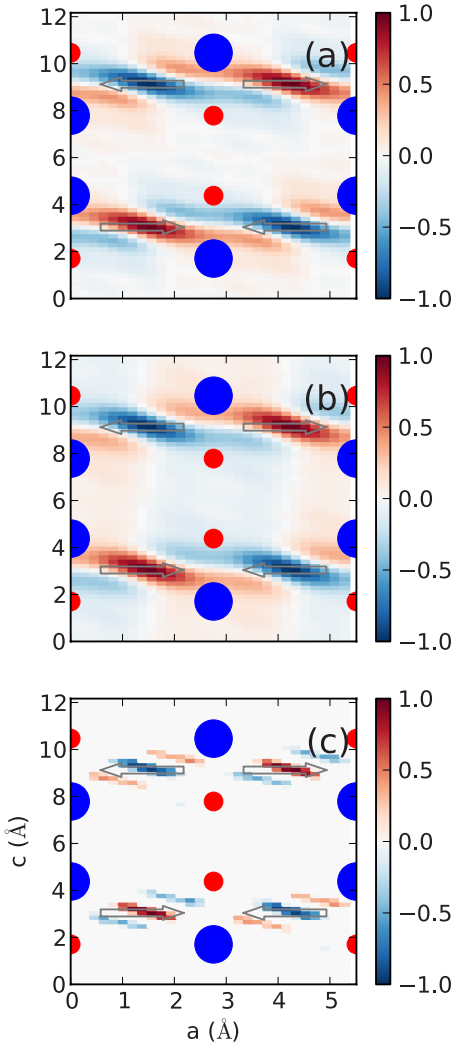

FIG. 2. (Color online) (a) Fourier inversion of the experimental form factor, yielding the projection of the magnetization density onto the *a*-*c* plane of the crystal structure. The different (red and blue) shaded regions with the arrows reversed indicate the oppositely directed magnetization of the antiferromagnetic structure. Note the elongation of the density along the Fe-As bond, indicated for the As ions above (small red circles) for one spin direction and below (large blue circles) the Fe plane for the other spin direction. (b) Magnetization density in the Fe plane obtained from the simulated data, where higher Q as well as $K \neq 0$ reflections have been calculated and included in the inversion. The similarity of the two plots demonstrates that the features obtained from the actual data are robust against termination effects and the absence of $K \neq 0$ data. (c) Maximum entropy reconstruction of the magnetization density, which also yields the same basic magnetization density. For all plots, the densities have been normalized.

along the nonelongated direction, which may also be an indication of bonding. It would be particularly interesting to determine if these features can be reproduced theoretically.

In general an electron in a solid has a wave function of the form $u(r)e^{i\mathbf{k}\cdot\mathbf{r}}$, where $u(r)$ must be compatible with the symmetry of the lattice but basically looks like an atomic wave function, s,p,d, etc. It should be noted that the shape of the wave function is unrelated to whether the electrons are localized or itinerant, and therefore a determination of the magnetic form factor does not address that question; itineracy is determined by whether or not the band crosses the Fermi surface. For the cuprates the single d electron hole has e_g symmetry, x^2-y^2, which is quite anisotropic and so makes the magnetic form factor anisotropic.[5] Moreover, the in-plane nearest-neighbor spins are aligned antiparallel, and therefore any net spin transferred onto the intervening oxygen ion cancels to first order, so that the effects of bonding are difficult to detect in magnetic form factor measurements. For K_2IrCl_6, on the other hand, the single electron on the Ir occupies a linear combination of t_{2g} orbitals, which again yields a quite anisotropic form factor.[6] It also gives rise to a noncollinear (atomic) spin density and separation of the charge and spin degrees of freedom. This latter property is amplified by the bonding to the Cl ions, where charge is transferred to all six Cl ions in the $IrCl_6$ complex but spin is transferred only to the two Cl ions that reside along the spin direction. This spin transfer onto the Cl is not cancelled by neighboring spins since the Cl are not shared, rendering the overall form factor highly anisotropic. This highly anisotropic behavior contrasts with the present iron-based superconductors, where band theory shows that all five d-bands are occupied and cross the Fermi energy. Therefore the magnetic electrons are itinerant in character, with a multiorbital description that is expected to yield a magnetic form factor that is much closer to isotropic (as observed). Note in particular that if the d bands have equal occupancies then the form factor has spherical symmetry. In the iron-based systems, however, any spin transferred to the As ion along the b-direction does not cancel since neighboring spins are parallel, making it easier to see these bonding effects. We also note that the in-plane exchange interactions are dramatically different along the a versus the b axis,[14–16] which should be related to the anisotropy of the projected spin-density distribution that has been determined here.

IV. STRUCTURAL PHASE TRANSITION

In the previous investigation of the structural phase transition, which breaks the high-temperature tetragonal symmetry in going to the low-temperature orthorhombic structure, the in-plane structure was characterized in detail.[7] The structural transition occurs rather abruptly, with the long-range antiferromagnetic order developing at the same temperature.[7,17] The shift in the diffraction peaks related to the structural distortion in the a-b plane were found to be symmetric, in that one crystal axis (a) increased while the other (b) decreased by the same amount. Thus there was no change in the area of the a-b plane. More recent studies in other systems[18] have found that the splitting can occur asymmetrically, concomitant with an abrupt change in the c-axis as well. Since the behavior of the c-axis lattice parameter through the transition was not determined in that study, we carried out high-resolution measurements of the (0,0,4) structural Bragg reflection to investigate whether there is any significant change in the c axis for $SrFe_2As_2$ in going through the phase transition. Figure 3 shows radial (θ:2θ) scans through this reflection, which provide a direct determi-

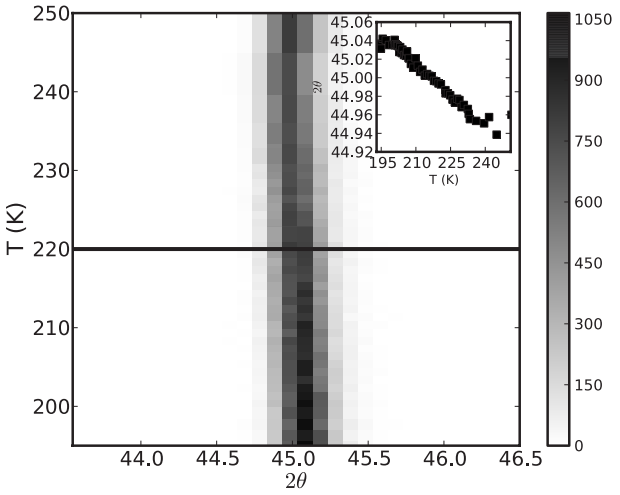

FIG. 3. Intensity of the (0,0,4) Bragg peak, as measured in a radial (θ:2θ) scan, as a function temperature. The black horizontal line represents the temperature of the tetragonal-orthorhombic transition at ~220 K. The inset shows the position of the reflection, which exhibits a smooth variation with temperature with no indication of a structural phase transition. In most cases, error bars are smaller than the marker size.

nation of the *c*-axis lattice parameter. The horizontal (black) line indicates the temperature of the structural phase transition. The intensity of the reflection is indicated by the shading, and the inset shows an expanded view of the temperature variation of the position of the reflection. There is some modest change in the intensity of the reflection and a smooth variation of the lattice parameter, but we clearly see that there is no abrupt change in the *c*-axis lattice parameter through the transition, in contrast to what is seen in $Ca(Fe\text{-}Ni)_2As_2$.[18] Combined with the previous results for the *a*-*b* plane,[7] we see that there is no detectable change in the volume of the unit cell for $SrFe_2As_2$ through the structural/magnetic phase transition.

V. CONCLUSIONS

In summary, we have measured the magnetic form factor in $SrFe_2As_2$, and found it to be approximately isotropic and in reasonable agreement with the form factor of metallic Fe. This behavior is consistent with electron occupancy of all five *d* orbitals as expected from band theory calculations. Both Fourier inversion of the data and maximum entropy reconstructions suggest an elongation of the moment densities in the direction of As atoms, indicative of Fe-As bonding. We have also investigated the behavior of the *c* axis through the structural phase transition, and found no significant anomaly as a function of temperature. This structural behavior differs from that observed in $Ca(Fe\text{-}Ni)_2As_2$, which exhibits an asymmetry in the in-plane distortion and an abrupt *c*-axis anomaly.

ACKNOWLEDGMENTS

The work at UT/ORNL is supported by the U.S. DOE, BES, through DOE Grant No. DE-FG02-05ER46202, and in part by the U.S. DOE, Division of Scientific User Facilities. The work at IOP, CAS is supported by CAS and 973 Program (Program No. 2010CB833102).

*Corresponding author.

[1] For a recent review see J. W. Lynn and P. Dai, Physica C **469**, 469 (2009).
[2] T. Yildirim, Physica C **469**, 425 (2009).
[3] C. Xu, M. Müller, and S. Sachdev, Phys. Rev. B **78**, 020501(R) (2008).
[4] For a recent review see D. J. Singh, Physica C **469**, 418 (2009).
[5] S. Shamoto, M. Sato, J. M. Tranquada, B. J. Sternlieb, and G. Shirane, Phys. Rev. B **48**, 13817 (1993).
[6] J. W. Lynn, G. Shirane, and M. Blume, Phys. Rev. Lett. **37**, 154 (1976).
[7] J. Zhao, W. Ratcliff II, J. W. Lynn, G. F. Chen, J. L. Luo, N. L. Wang, J. Hu, and P. Dai Phys. Rev. B **78**, 140504(R) (2008).
[8] S. W. Lovesey, *Theory of Neutron Scattering from Condensed Matter* (Oxford, New York, 1984), Vol. 2.
[9] W. Gavin Williams, *Polarized Neutrons* (Oxford, New York, 1988).
[10] R. M. Moon, Physica B **137**, 19 (1986); see also, *International Tables for Crystallography* (Kluwer Academic Publishers, Dordrecht, 1992), Vol. C, p. 392.
[11] R. J. Papoular and B. Gillon, Europhys. Lett. **13**, 429 (1990); A. Gukasov, M. Braden, R. J. Papoular, S. Nakatsuji, and Y. Maeno, Phys. Rev. Lett. **89**, 087202 (2002); A. Zheludev, R. J. Papoular, E. Ressouche, and J. Schweizer, Acta Crystallogr., Sect. A: Found. Crystallogr. **51**, 450 (1995).
[12] R. Andreani, E. G. Birgin, J. M. Martínez, and M. L. Schuverdt, SIAM J. Optim. **18**, 1286 (2007); Math. Program. **111**, 5 (2008).
[13] F. Izumi and R. A. Dilanian, *Recent Research Developments in Physics* (Transworld Research Network, Trivandrum, 2002), Vol. 3, Pt. II, p. 699.
[14] M. J. Han, Q. Yin, W. E. Pickett, and S. Y. Savrasov, Phys. Rev. Lett. **102**, 107003 (2009).
[15] A. Ong, G. S. Uhrig, and O. P. Sushkov, Phys. Rev. B **80**, 014514 (2009).
[16] J. Zhao, D. T. Adroja, D.-X. Yao, R. Bewley, S. Li, X. F. Wang, G. Wu, X. H. Chen, J. Hu, and P. Dai, Nat. Phys. **5**, 555 (2009).
[17] A. Jesche, N. Caroca-Canales, H. Rosner, H. Borrmann, A. Ormeci, D. Kasinathan, H. H. Klauss, H. Luetkens, R. Khasanov, A. Amato, A. Hoser, K. Kaneko, C. Krellner, and C. Geibel, Phys. Rev. B **78**, 180504(R) (2008).
[18] N. Kumar, S. Chi, Y. Chen, K. G. Rana, A. K. Nigam, A. Thamizhavel, W. Ratcliff II, S. K. Dhar, and J. W. Lynn, Phys. Rev. B **80**, 144524 (2009).
[19] Y. Lee, D. Vaknin, H. Li, W. Tian, J. L. Zarestky, N. Ni, S. L. Bud'ko, P. C. Canfield, R. J. McQueeney, and B. N. Harmon, Phys. Rev. B **81**, 060406(R) (2010).